

# Optimized triangular observer based adaptive supertwisting sliding mode control for wind turbine system

Sanae El Bouassi<sup>1</sup>, Youssef El Afou<sup>1</sup>, Zakaria Chalh<sup>1</sup>, El Mehdi Mellouli<sup>1</sup>, Touria Haidi<sup>2</sup>

<sup>1</sup>Laboratory of Engineering, System and Application, National School of Applied Sciences, Sidi Mohammed Ben Abdellah University, Fez, Morocco

<sup>2</sup>Laboratory of Systems Engineering, Hassania School of Public Works (EHTP), Casablanca, Morocco

## Article Info

### Article history:

Received Nov 28, 2023

Revised Mar 29, 2024

Accepted Apr 17, 2024

### Keywords:

Adaptive supertwisting sliding mode control

Lyapunov stability

Sliding mode control

Supertwisting mode control

Triangular observer

## ABSTRACT

This paper presents a modified adaptive supertwisting sliding mode controller (AST-SMC) that dynamically adjusts control settings without prior knowledge of uncertainty limits, thereby removing chattering and putting reliability first while maintaining the original benefits of sliding mode control (SMC). First, we model and build the wind turbine system using three different controllers: the AST-SMC, the supertwisting sliding mode controller (ST-SMC), and the first-order sliding mode controller (FOSMC). A second comparison is necessary. Only the rotor speed is available to the control law because of concealed state information, which makes use of the full system state. In order to minimize observing errors over time, an asymptotic observer triangle is used to estimate the unknown rotor acceleration. By improving AST-SMC's control law, particle swarm optimization finds the most effective controller. The stability of AST-SMC over a finite time is shown via the Lyapunov stability theorem. Based on simulation findings, it is proven to be more effective than traditional SMC in wind turbine system control. It excels in settling time, tracking accuracy, energy consumption, and control input smoothness.

*This is an open access article under the [CC BY-SA](https://creativecommons.org/licenses/by-sa/4.0/) license.*



## Corresponding Author:

Sanae El bouassi

Laboratory of Engineering, System and Application, National School of Applied Sciences

Sidi Mohammed Ben Abdellah University

Fez, Morocco

Email: sanae.elbouassi@usmba.ac.ma

## 1. INTRODUCTION

The recent years have seen a significant increase in interest in the generation of renewable energy, particularly in nations without access to natural energy resources and in response to the rapid rise in global energy demand and the threat of resource depletion [1], [2]. One of the major clean, renewable energy sources used to produce power is wind energy. Designing controls for nonlinear systems is difficult because practical control systems always incorporate nonlinear plants. In order to overcome the difficulty of developing a controller for a real system [3], the performance of wind turbine systems, noted for their inherent nonlinearity [4], [5], has been improved using a variety of nonlinear control approaches, such as the incorporation of sliding mode control (SMC) with artificial intelligence and various optimization techniques [6], [7].

Because of its straightforward design and capacity to offer a good control function, the supertwisting algorithm sliding mode controller (ST-SMC) [8]–[10] is a well-liked approach in high order sliding mode control (HOSMC) [11]. The ST-SMC cannot eliminate chattering while providing a continuous control action due to the discontinuous function under the integral action. Though theoretically higher gains should lead to higher ripples and system overshoot, in fact they actually lead to less effective disturbance suppression. This research offers an

adaptive supertwisting sliding mode controller (AST-SMC) based on the HOSMC scheme with adaptive gains for the auxiliary term contained in the second portion of the control law, which is inspired by the work published in [12]. The sliding variable's stability can be improved by using this method, which can reduce the sliding variable's derivative to zero under disturbance [13], [14]. This AST-SMC pushes control techniques to previously unheard-of levels of flexibility while preserving the best features of the classic SMC. It is similar to granting the controller real-time learning capabilities, which enable it to adjust and maximize performance on the fly, to be able to dynamically change control settings without having to know beforehand about uncertainty bounds.

The AST-SMC essentially takes on the role of a quiet sentinel, keeping a close eye on the system and precisely reacting to variations and uncertainties. This dynamic adaptability is a tactical advantage in the always-changing renewable energy market, not just a technical achievement. When a wind turbine system experiences abrupt variations in load or changes in wind patterns, traditional controllers may struggle to keep the system stable and efficient. In these situations, the AST-SMC performs admirably. To sum up, the AST-SMC is a dynamic maestro arranging harmony in the face of uncertainty, not merely a controller. It not only tackles the complexities of wind energy but also paves the way for a future where control systems are not just responsive but also intuitive and resilient in the face of uncertainty by maintaining the core principles of SMC while embracing adaptation.

The following is how this essay is structured: section 2 introduces the wind turbine system model, section 3 presents the first-order sliding mode controller (FOSMC) mathematical model that includes stability, convergence study, the ST-SMC, and AST-SMC based control laws' mathematical proofs, and derivations are described in sections 4 and 5, respectively. Section 5 also gives the stability analysis based on the Lyapunov theorem. Section 6 presents an asymptotic triangular observer and section 7 uses the particle swarm optimization (PSO) approach to improve an important gain in the control law. Section 9 brings the paper to a close.

## 2. WIND TURBINE MODELING

The following formulas [15], [16] can be used to determine the aerodynamic torque of a variable speed wind turbine. The Figure 1 illustrates a wind model with two masses. This schematic provides a conceptual framework for understanding the dynamics and forces involved in a system affected by wind by showing the interconnected relationship between the two masses.

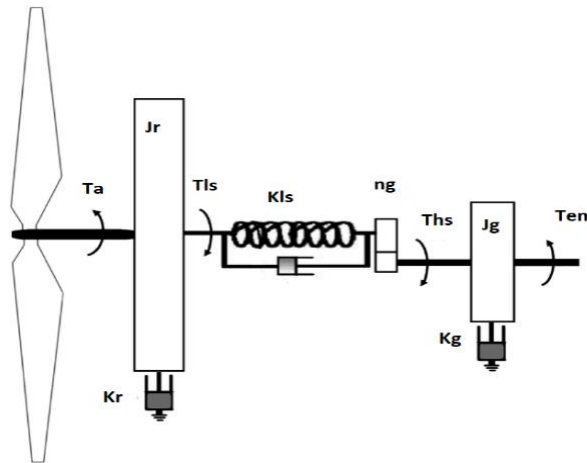


Figure 1. Wind model with two masses

$$T_a = \frac{1}{2} \rho \pi R^3 \frac{C_p(\lambda, \beta)}{\lambda(t)} v(t)^2 \quad (1)$$

Where  $V$  is the wind speed,  $\rho$  is the air density,  $R$  is the rotor radius, and  $C_p$  is the power coefficient where:

$$\lambda(t) = R \cdot \omega_t / v(t) \quad (2)$$

The dynamics of the rotor is governed by:

$$J_r \dot{w}_t = T_a - T_{ls} - k_r w_t \quad (3)$$

Inertia, external damping, and rotational speed of the rotor are successively represented by  $J_r$ ,  $k_r$ , and  $w_t$ . The generator's speed  $w_g$  is given by the following expression:

$$J_g \dot{w}_g = T_{hs} - k_g w_g - T_{em} \quad (4)$$

The generator's inertia and friction factor are  $J_g$  and  $k_g$ . We define  $n_g$  with the assumption of a perfect transmission.

$$n_g = \frac{T_{ls}}{T_{hs}} \quad (5)$$

### 3. CLASSICAL SLIDING MODE CONTROL DESIGN

The primary goal of the research is to develop a novel control law that maximizes wind energy capture. The power coefficient curve has a distinct maximum, which corresponds to the perfect amount of wind energy and the desired trajectory  $w_{topt}$  [17], [18].

$$y_r = w_{topt} = \frac{v(t) \lambda_{opt}}{R} \quad (6)$$

Figure 1 shows the system as being represented by [19]:

$$\begin{cases} \dot{w}_t = w_g \\ \dot{w}_g = \left( \frac{-k_g}{J_g} - \frac{J_g}{n_g J_g} \right) * w_g - \frac{k_r}{n_g J_g} * w_t + \frac{1}{J_g n_g} T_a + \left( -\frac{1}{J_r} * \frac{k_{ls}}{n_g J_g} \right) * u(x, t) \\ y_1 = w_t \end{cases} \quad (7)$$

The sources of the system's errors are as (8):

$$e = w_{topt} - w_t, \dot{e} = \dot{w}_{topt} - \dot{w}_t \quad (8)$$

The following provides the sliding surface [20]:

$$\sigma = \dot{e} + k * e \quad (9)$$

With  $k$  being positive. The sliding surface's derivative is provided as (10):

$$\dot{\sigma} = \ddot{e} + k * \dot{e} \quad (10)$$

The following gives the equivalent command:

$$u_{eq}(t) = \frac{1}{g} * (w_{topt}'' - f(x) + k * \dot{e}) \quad (11)$$

where,  $f(x, t) = \left( \frac{-k_g}{J_g} - \frac{J_g}{n_g J_g} \right) * x_2 - \frac{k_r}{n_g J_g} * x_1 + \frac{1}{J_g n_g} T_a$ . In order to better satisfy robustness criteria and absorb shocks, the switching control law is as (12):

$$u_{sw} = -k_d * \text{sign}(\sigma) \quad (12)$$

As a result, the control law of the approach is as (13) [21]:

$$T_{em} = \frac{1}{g} * (w_{topt}'' - f(x) + k * \dot{e}) - k_d * \text{sign}(\sigma) \quad (13)$$

#### 3.1. Stability analysis

We study the system's stability using the Lyapunov approach, which is as (14):

$$V = \frac{1}{2} * \sigma^2 \quad (14)$$

The requirement for the Lyapunov function derivative to be negative is critical for system stability.

$$\dot{V} = \dot{\sigma} * \sigma < 0 \quad (15)$$

In (12) and (13) allow us to write

$$\dot{V} = \sigma(\ddot{w}_{top} - f(x) - g * T_{em} + k * \dot{e}) \quad (16)$$

When we simplify this equation, we get:

$$\dot{V} = \sigma(-k * \text{sign}(\sigma)) \quad (17)$$

If  $k > 0$  then  $\dot{V} < 0$

#### 4. ADAPTIVE SUPERTWISTING SLIDING MODE CONTROL

The ST-SMC generates a continuous control action that reduces, but does not eliminate, the chattering caused by the discrete function under integral action. The ST-SMC is capable handling disturbances with constrained gradients and known borders, however calculating the disturbance boundary is difficult [22], [23]. As a result, when dealing with gain adjustment concerns, adaptive supertwisting is recommended. We investigate the same system in (7) with varied load disturbances and uncertainty in system characteristics given as (18):

$$\begin{cases} \dot{x}_1 = x_2 \\ \dot{x}_2 = f(x, t) + g \cdot u(x, t) + \frac{1}{10} * \frac{k_g}{J_g} \text{randn} \\ y_1 = x_1 \end{cases} \quad (18)$$

Taking  $\dot{\sigma} = 0$  acquires the analogous component, which is the same as (11):

$$u_{eq}(t) = \frac{1}{g} * (\ddot{w}_{top} - f(x) + k * \dot{e}) \quad (19)$$

And the control law of the AST-SMC is given by :

$$\begin{cases} T_{AST} = [U_{eq}(x, t) + u_1 + u_2] \\ u_1 = -\hat{\alpha} \sqrt{|\sigma(t)|} \text{sign}(\sigma(t)) \\ \dot{u}_2 = \frac{-\hat{\beta}}{2} \text{sign}(\sigma(t)) \end{cases} \quad (20)$$

The revised control law is described below, with the same component as in (11) as well as the new adaptive continuous component shown in (12):

$$\begin{aligned} T_{AST} = & \frac{1}{g} * (\ddot{w}_{top} - f(x) + k * \dot{e}) + [-\hat{\alpha} \sqrt{|\sigma(t)|} \text{sign}(\sigma(t)) \\ & - \hat{\beta} \int_0^t \text{sign}(\sigma(\tau)) d\tau] \end{aligned} \quad (21)$$

The gains  $\hat{\alpha}$  and  $\hat{\beta}$  are real numbers that represent adaptive limited gains are given as (22):

$$\begin{cases} \hat{\alpha} = \begin{cases} \sigma_\alpha \sqrt{n_1/2} & , \text{if } \sigma \neq 0 \\ 0 & , \text{if } \sigma = 0 \end{cases} \\ \hat{\beta} = 2\varpi\alpha \end{cases} \quad (22)$$

In addition, we will compare the suggested AST-SMC to previously proposed approaches in the literature. The AST-SMC will be compared with the SMC and ST-SMC [24].  $T_{ST}$  denotes the ST-SMC control law, which may be represented as (23):

$$\begin{cases} T_{ST} = [U_{eq}(x, t) + u_1 + u_2] \\ u_1 = -\alpha \sqrt{|\sigma(t)|} \text{sign}(\sigma(t)) \\ \dot{u}_2 = \frac{-\beta}{2} \text{sign}(\sigma(t)) \end{cases} \quad (23)$$

The revised control law is presented below, using the identical section from (11) and the continuous part from (22):

$$T_{ST} = \frac{1}{g} * (w_{t\ddot{o}pt} - f(x) + k * \dot{e}) + [-\alpha\sqrt{|\sigma(t)|} \text{sign}(\sigma(t)) - \beta \int_0^t \text{sign}(\sigma(\tau)) d\tau] \quad (24)$$

The STA SMC system is identical to (19) but differs only in the constant gain constants  $\alpha$  and  $\beta$ . The benefits are as follows:

- Model-free: the control systems mentioned in (19) and (22) are model-free in the sense that no model-specific dynamical information is required [23], [24]. In contrast to SMC, where it is more challenging to determine the dynamics of a complicated system, this property makes it more suitable for practical applications. Due to its nonlinear model-free nature, the AST-SMC has a faster convergence and smoother performance by design. Flexibility: for large systems, computing and in ST-SMC and the gain in SMC requires knowledge of an unknown upper boundary, which is a laborious and practically impossible process. The recommended AST-SMC method is adaptable and does not require understanding of the upper bound uncertainty. Chattering: as seen in (13), the arbitrary signum function remains in the ultimate control law, resulting in significant chattering in the turbine system. By continuously adjusting the control gains while maintaining limited time stability, the suggested AST-SMC may readily deal with the chattering problem.
- Flexibility: the computation of and in ST-SMC, as well as the gain in SMC, needs knowledge of an unknown upper boundary, which is a time-consuming and nearly impossible procedure for large systems. The suggested AST-SMC technique is flexible and does not necessitate knowledge of the upper bound uncertainty [25].
- Chattering: as seen in (13), the arbitrary signum function remains in the ultimate control law, resulting in significant chattering in the turbine system. By continuously adjusting the control gains while maintaining limited time stability, the suggested AST-SMC may readily deal with the chattering problem.

## 5. STABILITY ANALYSIS

As a result, the system's input-output dynamics are as (25):

$$\dot{\sigma} = \frac{\partial \sigma}{\partial t} + \frac{\partial \sigma}{\partial x} f(x) + \frac{\partial \sigma}{\partial x} g(x)u \quad (25)$$

The uncertain function  $\delta(x, t) \in \mathbb{R}$  exists and is provable by the (26):

$$\delta(x, t) = \delta_0(x, t) + \Delta\delta(x, t) \quad (26)$$

Where  $\delta_0(x, t) > 0$  is a recognized function and  $\Delta\delta(x, t)$  is a constrained disturbance so that

$$\dot{\sigma} = u_{eq}(t) + \left(1 + \frac{\Delta\delta(x, t)}{\delta_0(x, t)}\right) * \delta_0(x, t) * T_{AST} \quad (27)$$

Using the Lyapunov method, which is as follows, we investigate the stability of the system:

$$V = \frac{1}{2} * \sigma^2 \quad (28)$$

In (27) and (26) allow us to write:

$$\dot{V} = (\lambda + 4\omega^2) \left( |\sigma|^{\frac{1}{2}} \text{sign}(\sigma) \right)^2 + \left( \left(1 + \frac{\Delta\delta(x, t)}{\delta_0(x, t)}\right) u_2 \right)^2 - 4\omega |\sigma|^{\frac{1}{2}} \text{sign}(\sigma) \left(1 + \frac{\Delta\delta(x, t)}{\delta_0(x, t)}\right) u_2 + \frac{1}{2n_1} (\hat{\alpha} - \hat{\alpha}^*)^2 + \frac{1}{2n_2} (\hat{\beta} - \hat{\beta}^*)^2 \quad (29)$$

Where  $\hat{\alpha}^*, \hat{\beta}^*, n_1, n_2$  are positive unknown constants

$$\dot{V} \leq -\mathcal{E} V^{\frac{1}{2}} + \Gamma \quad (30)$$

Where  $\mathcal{E} = \min(\sigma_\alpha, \sigma_\beta)$  and

$$\Gamma = -|\hat{\alpha} - \hat{\alpha}^*| \left( \frac{1}{n_1} \hat{\alpha} - \frac{\sigma_\alpha}{\sqrt{2n_1}} \right) - |\hat{\beta} - \hat{\beta}^*| \left( \frac{1}{n_1} \hat{\beta} - \frac{\sigma_\beta}{\sqrt{2n_2}} \right) \quad (31)$$

Moreover, because the term  $\Gamma$  will eventually go close to zero if the parameters  $\hat{\alpha}$  and  $\hat{\beta}$  fulfill the adaptive law (20), the inequality is as follows:

$$\dot{V} \leq -\varepsilon V^{\frac{1}{2}} \quad (32)$$

## 6. TRIANGULAR OBSERVER

### 6.1. Proposition

An adaptive supertwisting sliding mode triangular observer [5] whose observation error approaches zero after a finite period of time can be stated as follows for the system model described in (18):

$$\begin{cases} \dot{\hat{w}}_t = \hat{w}_g + \lambda_1 \text{sign}(w_t - \hat{w}_t) \\ \dot{\hat{w}}_g = \hat{w}_g + \lambda_2 \text{sign}(\tilde{w}_g - \hat{w}_g) \end{cases} \quad (33)$$

where,

$$\tilde{w}_g = \hat{w}_g + \lambda_1 \text{sign}_1(w_t - \hat{w}_t) \quad (34)$$

and,

$$\tilde{w}_t = w_t \quad (35)$$

Such as  $\text{sign}_i$  is characterized by:

$$\text{sign}_i(\cdot) = \begin{cases} 0 & \text{if } \tilde{x}_j - \hat{x}_j \neq 0 \\ j \in [1, i] \\ \text{sign}(\cdot) & \text{elsewhere} \end{cases}$$

### 6.2. Proof

The observer error is given by:

$$\begin{cases} e_1 = w_t - \hat{w}_t \\ e_2 = w_g - \hat{w}_g \end{cases}$$

The observer error's dynamics are as follows:

$$\begin{aligned} \dot{e}_1 &= e_2 - \lambda_1 \text{sign}(w_t - \hat{w}_t) \\ \dot{e}_2 &= \frac{k_g}{J_g} (\hat{w}_g - w_g) - \lambda_2 \text{sign}(\tilde{w}_g - \hat{w}_g) \end{aligned}$$

#### 6.2.1. Step 1

We consider the Lyapunov function for the convergence in finite time.

$$v_1 = \frac{1}{2} e_1^2 \quad (36)$$

$$\dot{v}_1 = e_1 \dot{e}_1 = e_1 (e_2 - \lambda_1 \text{sign}(w_t - \hat{w}_t)) \quad (37)$$

If  $\lambda_1 > |e_2|_{\max}$ , then  $\dot{v}_1 < 0$

After a limited amount of time  $t_1$ , we acquire the convergence of  $e_1$  toward zero. The state arrives at the sliding surface after  $t_1$ , and on this surface:

$$e_2 = \lambda_1 \text{sign}(w_t - \hat{w}_t) \quad (38)$$

### 6.2.2. Step 2

Let us demonstrate the convergence of  $e_2$  in a finite amount of time while maintaining the step 1 convergence requirement. By selecting the Lyapunov function [17]:

$$v_2 = \frac{1}{2}(e_1^2 + e_2^2)$$

In step 1 for  $t > t_1$ , we have  $e_1 = 0$

$$\dot{v}_2 = e_2 \dot{e}_2 = e_2(-\lambda_2 \text{sign}(e_2)) \quad (39)$$

Then for  $\lambda_2 > 0$ , we obtain  $\dot{v}_2 < 0$ . After a certain amount of time  $t_2 > t_1$ , we acquire the convergence of  $e_2$  toward zero.

## 7. PARTICLE SWARM METHOD FOR OPTIMISATION

PSO method is an intelligent optimization method based on swarm mobility and intelligence. It uses a specific amount of particles to search for the best optimal solution while creating a swarm of moving particles during the search period. The goal that the particles must accomplish is the function that the objective function determines [18].

At iteration  $(t + 1)$ , the new update of each particle's velocity  $v_{ij}$  and position  $x_{ij}$  is determined using the formulas in (40) and (41):

$$v_{ij}(t + 1) = w \cdot v_{ij}(t) + C_1 \cdot R_1 (p_{ij}(t) - x_{ij}(t)) + C_2 \cdot R_2 (g_{ij}(t) - x_{ij}(t)) \quad (40)$$

$$x_{ij}(t + 1) = x_{ij}(t) + v_{ij}(t + 1) \quad (41)$$

Where the best position obtained by the particle  $i$  is  $p_{ij}$ , while the best position attained by the neighborhood is  $g_{ij}$ . The weighting coefficients are  $C_1$  and  $C_2$ . A uniform distribution in the range  $[0, 1]$  yielded the random numbers  $R_1$  and  $R_2$ . To maximize the coefficient  $\hat{\beta}$  of the control law in (20), we presented this strategy, with the starting condition to maintain being that  $\hat{\beta} > 0$  in each iteration [18].

Using the PSO algorithms and the specified values from Table 1, and following the completion of the previous step as stated in Algorithm 1. Table 1 shows the best fitness function and the ideal design parameters and Table 2 presents the optimized values of  $\hat{\beta}$ . In order to determine the ideal parameter at the lowest feasible cost,  $\gamma$  is employed to calculate the cost of each particle. The following is the process that combines the PSO and AST-SMC. To illustrate the proposed method, refer to Figure 2, which presents a diagram of the suggested approach.

### Algorithm 1. PSO applied to ASTA-SMC

```

Algorithm: PSO_LCSMC
Input:  $L_B$ ,  $U_B$ ,  $Imax$ , PSO parameters values
Output: best fitness function  $\gamma$ , optimal value  $\hat{\beta}$ 
PSO initialization
While (Iteration  $\leq$   $Imax$ ) do
  for  $P_{size}$  do
    Update inertial weight
    Velocity updates
    Position update
    Handling boundary
  end
  for  $P_{size}$  do
    Assign  $\hat{\beta}$  to the ASTA-SMC controller
    E error calculation
     $\gamma$  fitness function calculation
    Evaluating fitness
    Updating the best particle
  end
  Updating the best  $\gamma$  fitness and  $\hat{\beta}$ 
end
Return the best  $\gamma$  fitness function and the optimum  $\hat{\beta}$ 
end

```

Table 1. PSO algorithm settings

Parameters	Nomenclature	Value
$L_B / U_B$	parameters' lower- and upper-bounds	[100 110] and [120 150]
$I_{max}$	Maximum number of iterations	100
$P_{size}$	Population size	100
$W_{max}$ and $W_{min}$	Inertia weights	1 and 0.99
$C_1$ and $C_2$	Acceleration factors	2 and 2

Table 2. The controller's ideal design parameters

Design consistent and ideal controller fitness	Values
$\hat{\beta}$	126
Best fitness function $\gamma$	116,2945

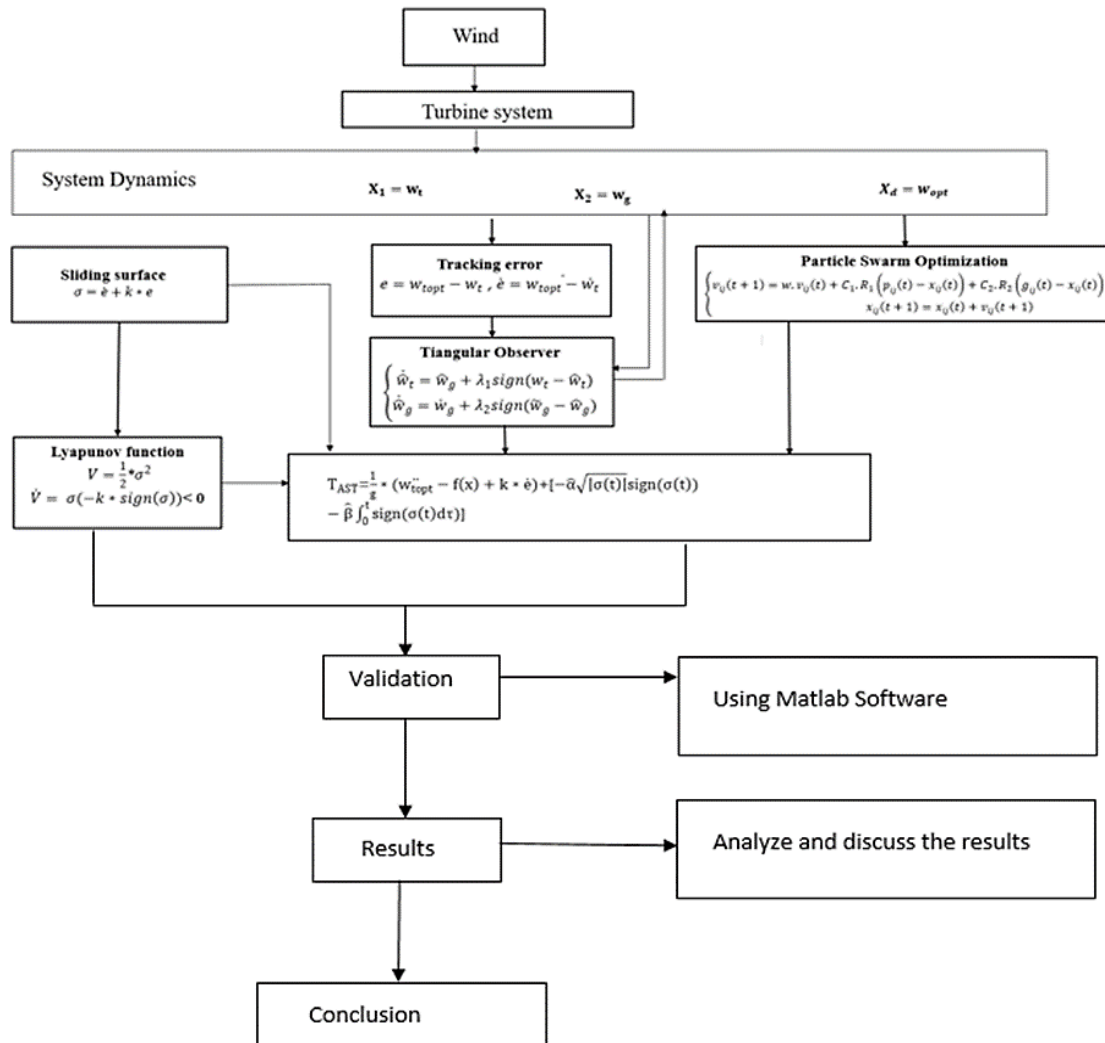


Figure 2. Diagram for suggested approach

## 8. SIMULATION RESULTS

The Figure 3 which presents the 4 curves of AST-SMC, SMC, and ST-SMC and the desired trajectory of the rotor speed, demonstrates how effective and swifter convergence occur when AST-SMC controller is used in system control. The following shows in Figure 4 depict how a wind turbine system behaves when utilizing AST-SMC with PSO. Following the estimation, we simulate the gain  $\hat{\beta}$  produced by the newly proposed AST-SMC method using PSO methodologies, to show the control law's evolution. These several simulations make it possible to compare the differences between the various controls, from which we infer that



AST-SMC with PSO is the most effective strategy because it was the first to converge showed in Figure 5. The triangular observer in Figure 6 permits to estimate the state  $x_2$ , which is in general unknown. The observer error, as illustrated in Figure 7, consistently converges toward zero, underscoring a high level of precision.

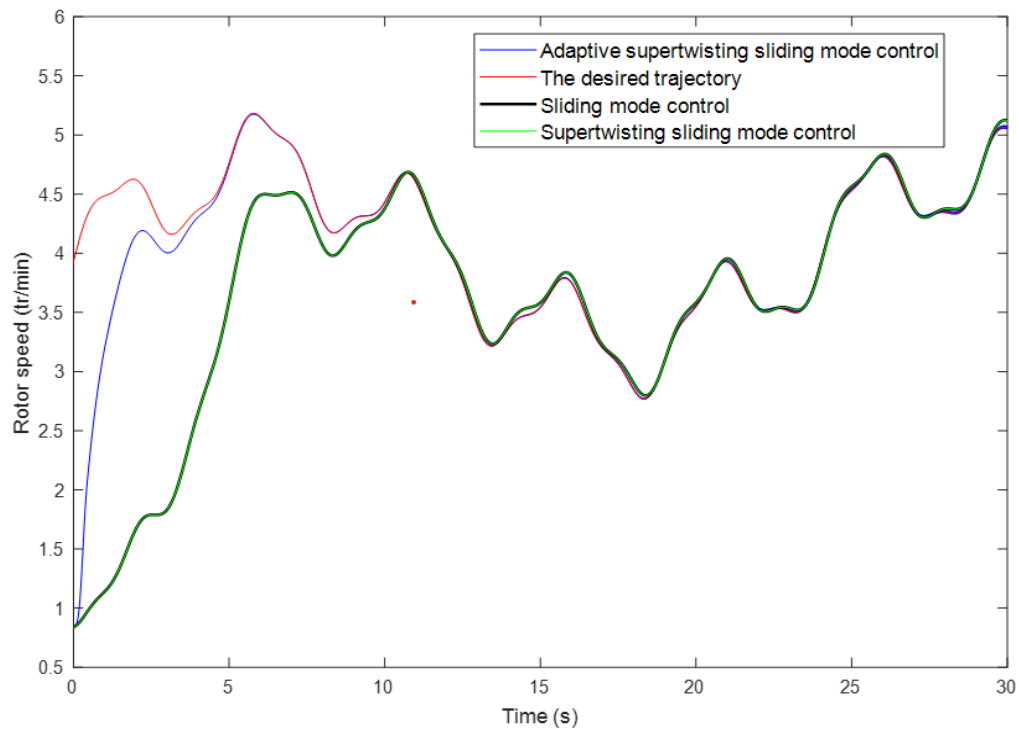


Figure 3. The comparison of the rotor speed obtained using SMC, AST-SMC, and ST-SMC

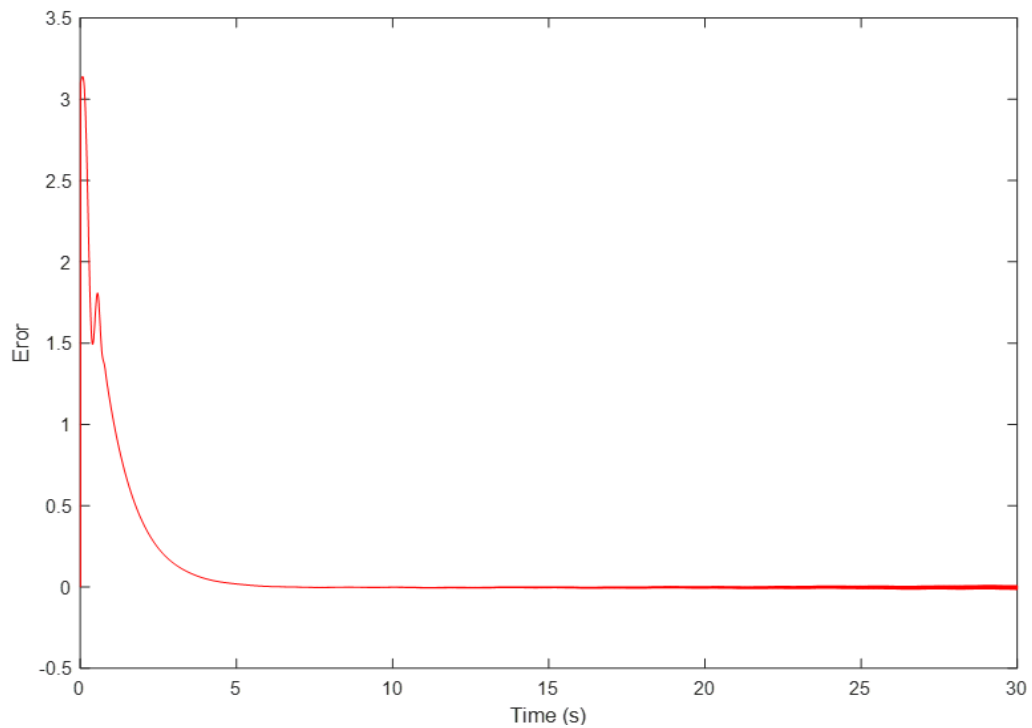


Figure 4. Rotor speed error utilizing AST-SMC

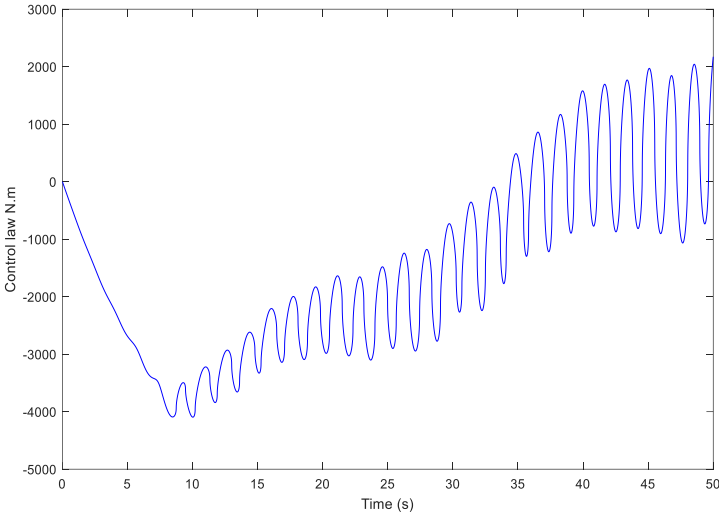


Figure 5. The response of the control law using PSO

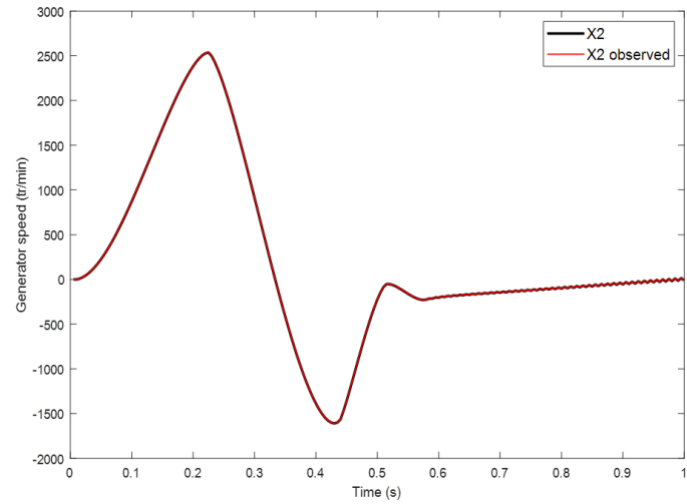


Figure 6. The behavior of  $x_2$  and  $\hat{x}_2$  observed

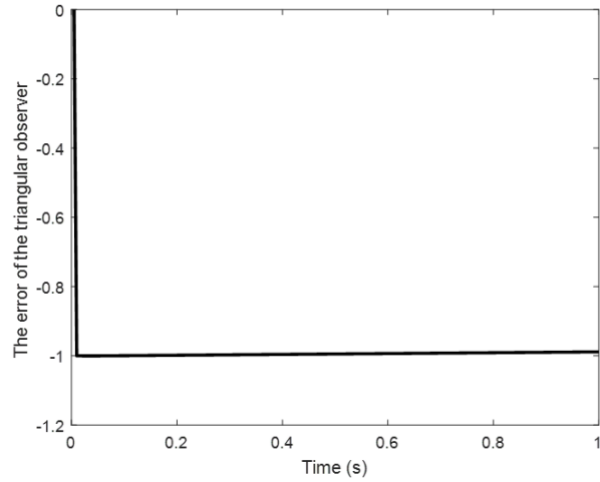


Figure 7. The triangular observer error

## 9. CONCLUSION

To approximate a function mechanism based on SMC for modeling and managing a wind turbine system, we introduced the AST-SMC in this study. To calculate the unknown rotor acceleration needed to construct the control law, a triangle observer is used. PSO is used to optimize key control law coefficients. When compared to the traditional SMC technique, this method's effectiveness is clear, and it improved when approximation approaches were used. To ensure the system's stability, the Lyapunov technique is utilized. Results thus demonstrate that the most accurate controller for complex systems is the AST-SMC with PSO approach. In this optics, we may make and search for other approximations and approaches to certain parameters and gains also using other controllers in order to enhance the performance and efficiency of our system. This strategy is consistent with a more general notion of control system adaptability and continual improvement. We improve the existing system and set the stage for future improvements by taking into account a range of controllers and methods. Dynamic solutions are required in the ever-changing renewable energy sector, and investigating various approximations and controller methodologies is a proactive step toward attaining long-term performance and efficiency increases in our wind turbine system.




## REFERENCES

- [1] A. Sellami, D. Arzelier, R. M'hiri, and J. Zrida, "A sliding mode control approach for systems subjected to a norm-bounded uncertainty," *International Journal of Robust and Nonlinear Control*, vol. 17, no. 4, pp. 327–346, 2007, doi: 10.1002/rnc.1140.
- [2] A. G. Aissaoui, A. Tahour, M. Abid, N. Essounbouli, and F. Nollet, "Power control of wind turbine based on fuzzy controllers," *Energy Procedia*, vol. 42, pp. 163–172, 2013, doi: 10.1016/j.egypro.2013.11.016.
- [3] C. Chatri, M. Ouassaid, M. Labbadi, and Y. Errami, "Integral-type terminal sliding mode control approach for wind energy conversion system with uncertainties," *Computers and Electrical Engineering*, vol. 99, Apr. 2022, doi: 10.1016/j.compeleceng.2022.107775.
- [4] J. Mérida, L. T. Aguilar, and J. Dávila, "Analysis and synthesis of sliding mode control for large scale variable speed wind turbine for power optimization," *Renewable Energy*, vol. 71, no. 11, pp. 715–728, 2014, doi: 10.1016/j.renene.2014.06.030.
- [5] Y. Li, Z. Xu, and K. Meng, "Optimal power sharing control of wind turbines," *IEEE Transactions on Power Systems*, vol. 32, no. 1, pp. 824–825, 2017, doi: 10.1109/TPWRS.2016.2549741.
- [6] H. Chen *et al.*, "Adaptive super-twisting control of doubly salient permanent magnet generator for tidal stream turbine," *International Journal of Electrical Power and Energy Systems*, vol. 128, 2021, doi: 10.1016/j.ijepes.2021.106772.
- [7] W. Du, G. Yang, C. Pan, P. Xi, and Y. Chen, "A sliding-mode-based duty ratio controller for multiple parallelly-connected DC–DC converters with constant power loads on MVDC shipboard power systems," *Energies*, vol. 13, no. 15, 2020, doi: 10.3390/en13153888.
- [8] I. Sami, A. Abid, N. Khan, M. M. Zaid, H. Ahmad, and H. Ali, "Supertwisting sliding mode control of multi-converter MVDC power systems under constant power loads," *2021 IEEE 4th International Conference on Computing, Power and Communication Technologies (GUCon)*, Kuala Lumpur, Malaysia, 2021, pp. 1–5, doi: 10.1109/GUCon50781.2021.9573535.
- [9] Y. Shtessel, M. Taleb, and F. Plestan, "A novel adaptive-gain supertwisting sliding mode controller: methodology and application," *Automatica*, vol. 48, no. 5, pp. 759–769, 2012, doi: 10.1016/j.automatica.2012.02.024.
- [10] F. Qiao, Q. Zhu, A. F. Winfield, and C. Melhuish, "Adaptive sliding mode control for MIMO nonlinear systems based on fuzzy logic scheme," *International Journal of Automation and Computing*, vol. 1, no. 1, pp. 51–62, 2004, doi: 10.1007/s11633-004-0051-4.
- [11] W. Zhang and L. Zhao, "Survey and tutorial on multiple model methodologies in modelling, identification and control," *International Journal of Modelling, Identification and Control*, vol. 32, no. 1, pp. 1–9, 2019, doi: 10.1504/IJMIC.2019.101955.
- [12] B. Wang, T. Wang, Y. Yu, C. Luo, and D. Xu, "Convergence trajectory optimization of supertwisting sliding-mode current control for induction motor drives," *IEEE Transactions on Industrial Electronics*, vol. 69, no. 12, pp. 12292–12304, 2022, doi: 10.1109/TIE.2021.3130328.
- [13] S. El Bouassi, Z. Chalh, and E. M. Mellouli, "A new robust adaptive control for variable speed wind turbine," *Lecture Notes in Networks and Systems*, vol. 635, pp. 90–96, 2023, doi: 10.1007/978-3-031-26254-8\_13.
- [14] Y. Soufi, S. Kahla, and M. Bechouat, "Particle swarm optimization based sliding mode control of variable speed wind energy conversion system," *International Journal of Hydrogen Energy*, vol. 41, no. 45, pp. 20956–20963, 2016, doi: 10.1016/j.ijhydene.2016.05.142.
- [15] M. Ayadi, O. Naifar, and N. Derbel, "High-order sliding mode control for variable speed PMSG-wind turbine-based disturbance observer," *International Journal of Modelling, Identification and Control*, vol. 32, no. 1, pp. 85–92, 2019, doi: 10.1504/IJMIC.2019.101958.
- [16] M. -Fuentes, C. Arturo, R. Seeber, L. Fridman, and J. A. Moreno, "Saturated lipschitz continuous sliding mode controller for perturbed systems with uncertain control coefficient," *IEEE Transactions on Automatic Control*, vol. 66, no. 8, pp. 3885–3891, 2021, doi: 10.1109/TAC.2020.3034872.
- [17] J. Mérida, L. T. Aguilar, and J. Dávila, "Analysis and synthesis of sliding mode control for large scale variable speed wind turbine for power optimization," *Renewable Energy*, vol. 71, pp. 715–728, 2014, doi: 10.1016/j.renene.2014.06.030.
- [18] A. Norouzi, R. Kazemi, and S. Azadi, "Vehicle lateral control in the presence of uncertainty for lane change maneuver using adaptive sliding mode control with fuzzy boundary layer," in *Proceedings of the Institution of Mechanical Engineers. Part I: Journal of Systems and Control Engineering*, 2018, vol. 232, no. 1, pp. 12–28, doi: 10.1177/0959651817733222.
- [19] Z. El Idrissi, T. Haidi, F. Elmariami, and A. Belfqih, "Comparative study of optimization methods for optimal coordination of directional overcurrent relays with distributed generators," *IAES International Journal of Artificial Intelligence*, vol. 12, no. 1, pp. 209–219, 2023, doi: 10.11591/ijai.v12.i1.pp209-219.
- [20] A. S. Rawat, A. Rana, A. Kumar, and A. Bagwari, "Application of multi layer artificial neural network in the diagnosis system: a systematic review," *IAES International Journal of Artificial Intelligence*, vol. 7, no. 3, pp. 138–142, 2018, doi: 10.11591/ijai.v7.i3.pp138-142.
- [21] T. Y. Lee, "Short term hydroelectric power system scheduling with wind turbine generators using the multi-pass iteration particle swarm optimization approach," *Energy Conversion and Management*, vol. 49, no. 4, pp. 751–760, 2008, doi: 10.1016/j.enconman.2007.07.019.
- [22] W. Yang, H. Yue, E. Deng, "Comparison of aerodynamic performance of high-speed train driving on tunnel-bridge section under fluctuating winds based on three turbulence models," *Journal of Wind Engineering and Industrial Aerodynamics*, vol. 228, 2016, doi: 10.1016/j.jweia.2022.105081.




- [23] P. S. Babu, D. Hernandez, B. Bandyopadhyay, and L. Fridman. "A lipschitz continious sliding mode control for implicit systems," *European Journal of Control*, vol. 67, 2022, doi : 10.1016/j.ejcon.2022.100661.
- [24] S. Chehaidi, H. Kherfane, H. Cherif, "Robust nonlinear terminal integral sliding mode control for wind turbine considering uncertainties," *IFAC-PapersOnline*, 2022, doi: 10.1016/j.ifacol.2022.07.316.
- [25] Y. Li, Z. Xu and K. Meng, "Optimal Power Sharing Control of Wind Turbines," in *IEEE Transactions on Power Systems*, vol. 32, no. 1, pp. 824-825, Jan. 2017, doi: 10.1109/TPWRS.2016.2549741.

## BIOGRAPHIES OF AUTHORS






**Sanae El Bouassi**    graduated with a degree in electrical engineering from Hassania School of Public Works, Casablanca, Morocco in 2020. Currently, she is a Ph.D. Her research interests include renewable energy, wind turbine system control, particle swarm optimisation, power distribution protection, artificial intelligence, and nonlinear system. She can be contacted at email: [sanae.elbouassi@usmba.ac.ma](mailto:sanae.elbouassi@usmba.ac.ma).






**Youssef El Afou**    earned a Doctorate in Physics and specialization in Automatics from UMI and USTL1 between 2009 and 2014. His notable contributions include groundbreaking research on controlling climatic parameters in greenhouse environments. He is a proud recipient of a specialized Master's degree from ESA, obtained between 2007 and 2009. Currently serving as an Enseignant Chercheur at the Ecole Nationale des Sciences Appliquées, he continues to make significant strides in research and education, showcasing his multidisciplinary expertise in physics and automatics. He can be contacted at email: [youssef.elafou@usmba.ac.ma](mailto:youssef.elafou@usmba.ac.ma).






**Zakaria Chalh**    received his M.Sc. in Automatic and his Ph.D. in control and automation from Lille University's Centrale Graduate School in 2008. Since 2011, he has served as an instructor and the head of the industrial division at Fez University, which houses Morocco's National School of Applied Sciences. His works have been published in more than 20 prestigious international journals and conferences. His areas of interest in research include modeling, identification, resilient controls, multidimensional systems, intelligent controls, and bond graphs. He can be contacted at email: [zakaria.chalh@usmba.ac.ma](mailto:zakaria.chalh@usmba.ac.ma).



**El Mehdi Mellouli**    earned his master's degree in 2008 from the University Sidi Mohamed Ben Abdellah, Faculty of Sciences in Fes. He graduated from the Moroccan Fez University with a degree in robotics and fuzzy control. Fuzzy control systems, sliding mode control, nonlinear systems, automatic control of industrial processes, modeling, and simulator creation were the main topics of his Ph.D. work. Numerous of his papers have appeared in renowned international journals. He can be contacted at email: [mellouli\\_elmehdi@hotmail.com](mailto:mellouli_elmehdi@hotmail.com).



**Touria Haidi**    received a degree in Electrical Engineering in 1988 from EHTP, Casablanca, Morocco, a post-graduate certificate in information processing in 1992 from Ben Msick, University Hassan II, a Specialized Master in Information Systems in 2005 from EHTP and a Habilitation to University Research (HDR) in 2018 from ENSEM. Currently, she is a Professor of Electrical Engineering at EHTP and teaches Electrical Engineering and Electrical Machines. Her researches are focused on renewable energy and electrical networks. She can be contacted at email: [touriahaidi60@gmail.com](mailto:touriahaidi60@gmail.com).